Materials Science Forum Vol. 729 (2013) pp 228-233

doi:10.4028/www.scientific.net/MSF.729.228

Microstructure and thermal stability of copper - carbon nanotube composites consolidated by High Pressure Torsion

P. Jenei[1,a], E.Y. Yoon[2,b], J. Gubicza[1,c], H.S. Kim[2,d], J.L. Lábár[1,3,e], T. Ungár[1,f]

[1]Department of Materials Physics, Eötvös Loránd University Budapest, P.O.B. 32, H-1518, Hungary
[2]Department of Materials Science and Engineering, Pohang University of Science and Technology, Pohang, Korea
[3]Institute for Technical Physics and Materials Science, Research Centre for Natural Sciences, P.O.Box 49, H-1525 Budapest, Hungary
[a]jeneip22@freemail.hu (corresponding author), [b]eyyoon@postech.ac.kr, [c]gubicza@metal.elte.hu, [d]hskim@postech.ac.kr, [e]labar.janos@ttk.mta.hu, [f]ungar@ludens.elte.hu

Keywords: Carbon nanotube, High-pressure torsion, Microstructure, Hardness, Thermal stability.

Abstract. Blends of Cu powders and 3 vol. % carbon nanotubes (CNTs), and an additional sample from pure Cu powder were consolidated by High Pressure Torsion (HPT) at room temperature (RT) and 373 K. The grain size, the lattice defect densities as well as the hardness of the pure and composite materials were determined. Due to the pinning effect of CNTs, the dislocation density is about three times larger, while the grain size is about half of that obtained in the sample consolidated from the pure Cu powder. The increase of the HPT-processing temperature from RT to 373 K resulted in only a slight increase of the grain size in the Cu-CNT composite while the dislocation density and the twin boundary frequency were reduced significantly. The flow stress obtained experimentally agrees well with the value calculated by the Taylor-formula indicating that the strength in both pure Cu and Cu-CNT composites is determined mainly by the interaction between dislocations. The addition of CNTs to Cu yields a significantly better thermal stability of the UFG matrix processed by HPT.

Introduction

Ultrafine-grained (UFG) microstructures in bulk metals can be produced by "bottom-up" or "top-down" methods. In the course of "bottom-up" procedures the materials are built up from individual atoms, molecules or their clusters (particles), such in electrodeposition or sintering processes. In the case of "top-down" methods, severe plastic deformation (SPD) is applied in order to refine the microstructure in coarse-grained bulk materials [1,2]. High Pressure Torsion (HPT) is a technique that has been applied mostly in the grain-refinement of bulk materials, but it is also capable for the consolidation of metallic powders [2]. In HPT-processing a thin disk is subjected to torsional straining under a high hydrostatic pressure. Besides single phase metals, HPT has been also used to fabricate metal–matrix nanocomposites [3,4]. Carbon nanotubes (CNTs) are promising disperse phase in these composites because their high strength and aspect ratio yield an enhancement of the mechanical behavior and thermal stability of the UFG matrix [3,4]. In this study, the influence of CNTs on the microstructure and hardness of UFG Cu processed by HPT at room temperature (RT) and 373 K is investigated. The thermal stability of the composite samples is compared with that for pure UFG Cu consolidated from a powder or processed from coarse-grained bulk material by HPT.

Experimentals

Sample preparation. Cu-CNT composites were produced from a 99.5% purity copper powder with particle sizes less than 44 μm (325 mesh, manufacturer: Chang Sung Co., Korea) and 3 vol.% multi-walled carbon nanotubes (MWCNTs) having a diameter and length of 5-20 nm and 1-10 μm, respectively (manufacturer: Applied Carbon Nano Co., Korea). In order to achieve a homogeneous

dispersion of MWCNTs in the Cu powder, their mixture was high-energy ball milled with stainless steel balls under an argon atmosphere. The powder blend was pre-compacted by cold isostatic pressing. The pre-compacted discs were finally consolidated by HPT at RT or 373 K with an applied pressure and number of revolution of 2.5 GPa and 10, respectively. The HPT-processed disks were 20 mm in diameter and 0.7 mm in thickness. For the purpose of comparison, two additional pure Cu samples were produced by 10 revolutions of HPT. The first specimen was consolidated at RT from the same pure Cu powder and under the same conditions as for the composite sample. The second specimen was processed from a bulk coarse-grained oxygen-free copper with 99.98 % purity by HPT under 4 GPa for 10 revolution at RT. In the following, the samples processed from bulk Cu, pure Cu powder, blend of Cu and CNTs at RT and 373 K are denoted as bulk-Cu, Cu, Cu-CNT-RT and Cu-CNT-373, respectively.

Characterization methods. The microstructure of the HPT-processed samples was examined at the center, half-radius and periphery by X-ray line profile analysis. The measurements of the X-ray diffraction lines were performed using a special high-resolution diffractometer (Nonius FR591) with CuKα_1 radiation (λ = 0.15406 nm). The line profiles were evaluated using the extended Convolutional Multiple Whole Profile (eCMWP) fitting procedure [5,6]. This method gives the crystallite size distribution as well as both the dislocation density and the twin boundary frequency with good statistics, where the latter quantity is defined as the relative fraction of twin boundaries among {111} lattice planes. The thermal stability of the HPT-processed samples were investigated by differential scanning calorimetry (DSC) using a Perkin-Elmer DSC2 calorimeter at a heating rate of 40 K/min. The grain structure was studied using a JEOL-200EX transmission electron microscope (TEM) operating at 200 kV. The morphology of CNTs after HPT was investigated by high resolution TEM (HRTEM) carried out by a JEOL-3010 transmission electron microscope operating at 300 kV. The TEM foils were prepared at the half-radius of the HPT-processed disks. In order to measure the remaining porosity in the consolidated samples, the cross-sections of the HPT-processed discs were polished and inspected by an FEI Quanta 3D scanning electron microscope (SEM). The porosity was determined as the area fraction of the pores at the center, half-radius and periphery of the disks. The microhardness was measured using a Zwick Roell ZHμ Vickers indenter with an applied load of 500 g and a dwell time of 10 s.

Results and discussion

Phase composition and porosity. The phase composition of the consolidated samples was studied by X-ray diffraction using the same device as for X-ray line profile analysis. In the center regime of the composite samples a small amount of Cu_2O was detected. In other parts of the discs oxide phase was not observed. The oxidation probably occurred during the ball milling. The oxide phase may be decayed due to severe plastic deformation by HPT, that can explain its absence at the half-radius and the periphery of the disks where the imposed strain is much higher than in the center. The morphology and the dispersion of CNTs in the matrix were studied by HRTEM. Complete CNTs were not observed, at the same time some graphite-like fragments were revealed from the interlayer spacings (about 0.34 nm) determined in the HRTEM images. The fragmentation of CNTs probably occured during high-energy milling and HPT-processing. As an example, Fig. 1a shows a HRTEM image of sample Cu-CNT-RT, where the arrows indicate fragments of MWCNTs. It should be noted, that neither CNT nor graphite peak was observed on the X-ray diffractograms of the composite samples due to the very small amount and size of nanotube fragments.

Fig. 1b shows a SEM image taken at the half-radius of sample Cu-CNT-373, where the dark spots indicate pores. The pores are randomly distributed with the size between 20 and 200 nm. The porosity values determined from the SEM images are listed in Table 1. The porosity in the Cu-CNT composite samples is about 2-3 % that is much higher than for the specimen consolidated from pure Cu powder (~0.5 %). These values are very close to the porosity calculated from the comparison of the theoretical and experimental mass densities measured by Archimedes' principle [7].

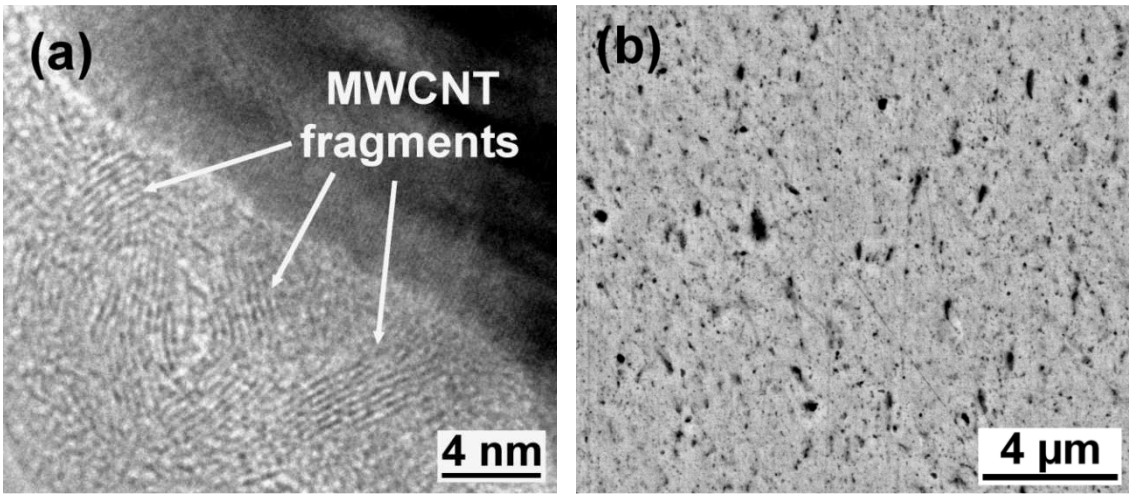

Figure 1. (a) High-resolution TEM image obtained at the half-radius of disk Cu-CNT-RT and (b) a SEM image of the polished cross-section at the half-radius of sample Cu-CNT-373.

Microstructure and microhardness. The microhardness was measured along the radius of the HPT discs with the step size of 1 mm. It was shown in a recently published paper [7] that the hardness increased with increasing the distance from the center and reached a saturation value at about 2 mm for all the four samples. The parameters of the microstructure and the microhardness at the center, half-radius and periphery of the HPT-processed discs are listed in Table 1. It can be concluded, that the dislocation density and the twin boundary frequency are smaller while the crystallite size is larger in the center than at the half-radius or periphery for all the samples. The smaller defect density and the hardness in the center can be explained by the smaller strain imposed during HPT. As the hardness investigation suggests that the microstructure saturated already at about 20 % of the radius for all the samples, therefore for comparison purpose it is reasonable to use the values of the microstructural parameters measured at the half-radius.

Figs. 2a and b show dark-field TEM images taken at the half-radius of specimens Cu and Cu-CNT-RT, respectively. The grain size in the composite sample is about half of the value obtained for pure Cu. The dislocation density and the mean crystallite size are significantly higher and smaller, respectively, at the half-radius in specimen Cu-CNT-RT than for the consolidated Cu sample. The larger defect density in sample Cu-CNT-RT can be explained by the pinning effects of CNT fragments on lattice defects. In sample Cu-CNT-RT a high twin boundary frequency was observed in contrast to pure Cu that can be explained by the hindering effect of CNT fragments on the escape of dislocations from pile-ups resulting in high stresses at glide obstacles. If the local stresses reach the critical value of twin nucleation, deformation twins are formed.

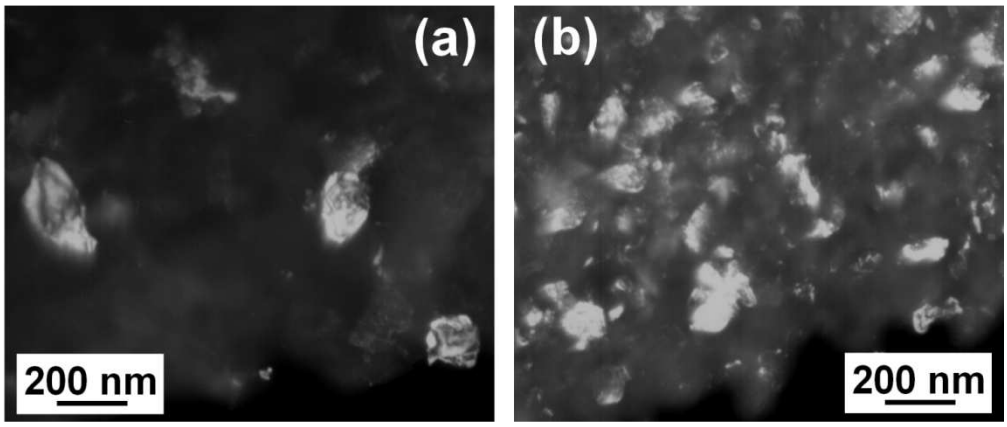

Figure 2. Dark-field TEM images for samples (a) Cu and (b) Cu-CNT-RT.

Due to the easier annihilation of lattice defects during HPT at 373 K, the dislocation density and the twin boundary frequency are much lower, while the mean crystallite and grain sizes are higher in specimen Cu-CNT-373 compared to sample Cu-CNT-RT. No significant difference between the parameters of the microstructure in Cu specimens consolidated from a powder or processed from a coarse-grained bulk material by HPT was observed. It seems that the saturation values of the microstructural parameters in pure Cu obtained by HPT-processing are not very sensitive to whether the initial material is bulk or powder.

Table 1. The microhardness (*HV*), the porosity (*P*), the grain size obtained by TEM (*d*), the area-weigthed mean crystallite size ($\langle x \rangle_{area}$), the dislocation density (ρ) and the twin boundary frequency (β) at the center, half-radius and periphery of the HPT-processed bulk-Cu, Cu, Cu-CNT-RT and Cu-CNT-373 discs.

Sample	*HV* [GPa]	*P* [vol. %]	*d* [nm]	$\langle x \rangle_{area}$ [nm]	ρ [10^{14} m^{-2}]	β [%]
Bulk-Cu, center	1.43 ± 0.04	0		66 ± 7	29 ± 3	0.0 ± 0.1
Bulk-Cu, half-radius	1.59 ± 0.05	0	160	57 ± 6	42 ± 4	0.0 ± 0.1
Bulk-Cu, periphery	1.55 ± 0.05	0		58 ± 6	43 ± 4	0.0 ± 0.1
Cu, center	1.46 ± 0.04	0.6		70 ± 7	36 ± 4	0.0 ± 0.1
Cu, half-radius	1.73 ± 0.05	0.5	174	60 ± 6	43 ± 4	0.0 ± 0.1
Cu, periphery	1.73 ± 0.05	0.5		61 ± 6	44 ± 4	0.0 ± 0.1
Cu-CNT-RT, center	1.26 ± 0.04	1.8		61 ± 6	31 ± 3	0.3 ± 0.1
Cu-CNT-RT, half-radius	2.31 ± 0.07	2.2	74	36 ± 4	111 ± 10	1.1 ± 0.1
Cu-CNT-RT, periphery	2.25 ± 0.07	1.5		35 ± 4	101 ± 10	1.1 ± 0.1
Cu-CNT-373, center	1.27 ± 0.04	3.3		56 ± 6	37 ± 4	0.2 ± 0.1
Cu-CNT-373, half-radius	1.81 ± 0.05	2.6	83	49 ± 5	66 ± 8	0.3 ± 0.1
Cu-CNT-373, periphery	1.76 ± 0.05	1.6		48 ± 5	53 ± 6	0.4 ± 0.1

The parameters of the microstructure and the flow stress determined from the hardness (*HV*) can be correlated using the Taylor and/or Hall-Petch formulas. In the former case, the flow stress (σ) corrected with the porosity (*P*) [8] is calculated from the dislocation density (ρ) as:

$$\sigma = \left(\sigma_0 + \alpha M^T G b \rho^{1/2}\right) \exp(-0.05P) , \quad (1)$$

where σ_0 is the friction stress (35 MPa [9]), α is a constant (0.22 [10]), *G* is the shear modulus (47 GPa [11]), *b* is the length of the Burgers vector (0.256 nm) and M^T is the Taylor factor (3.06 is selected as strong texture was not observed in the samples). The flow stress can also be related to the grain size (*d*) using the Hall-Petch equation corrected for porosity:

$$\sigma = \left(\sigma_0 + k d^{-1/2}\right) \exp(-0.05P) , \quad (2)$$

where *k* is the Hall-Petch slope (0.13 MPa·$m^{1/2}$ [12]). The flow stress calculated from eqs. (1) and (2) versus the measured values obtained as *HV*/3 are plotted in Fig 3a. It seems that the flow stresses determined from the Hall-Petch formula are much less than the experimental values. This is in accordance with previous observations for Cu-CNT composites [3,4]. At the same time, Fig. 4a reveals that the Taylor-equation is capable solely to estimate the strength of the microstructure in all samples. Most probably, in the HPT-processed specimens the majority of the grain boundaries are built up from dislocations and Orowan loops were formed around the nanotube fragments.

Therefore, the hardening effects of the grain boundaries and the CNTs can be regarded as interactions between dislocations [13] and consequently they are included in the Taylor-equation. This observation suggests that the CNT fragments in the Cu matrix have no direct strengthening effect, but rather they harden via the increase of the dislocation density.

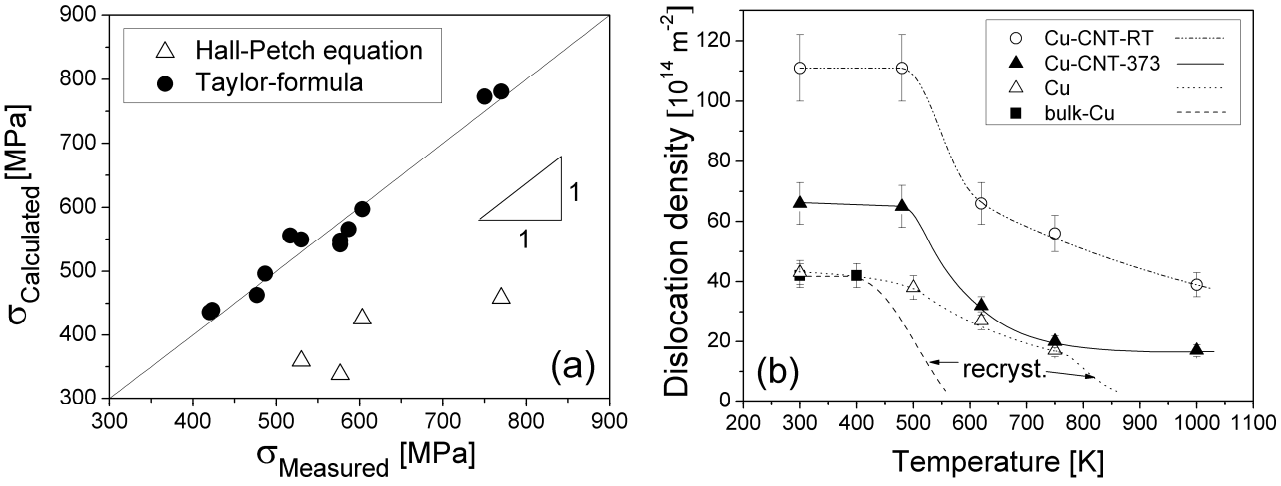

Figure 3. (a) Calculated flow stress as a function of the measured values. (b) The dislocation density as a function of temperature in DSC annealing at a heating rate of 40 K/min.

Thermal stability. In order to compare the thermal stability, the specimens were heated up to different temperatures in a DSC at a rate of 40 K/min, and then quenched to RT. The samples were cut from the discs at the half-radius. After the heat treatments the mean crystallite size, the dislocation density and the twin boundary frequency were determined using X-ray line profile analysis. Fig. 3b illustrates the difference in thermal stability of the samples by plotting the dislocation density as a function of annealing temperature. For the pure Cu specimens processed from powder or bulk material by HPT, the dislocation density remained unchanged up to about 500 or 400 K, respectively, then it decreased. It was observed from the Debye-Scherrer diffraction rings that a recrystallization also started at about 800 and 500 K for the consolidated and the bulk Cu, respectively. Therefore, despite the similar microstructures, the UFG Cu sample produced by powder metallurgy shows better thermal stability than the specimen processed from bulk Cu by HPT. Most probably, this difference can be attributed to impurities and oxide which are usually unavoidable in powder metallurgy [14]. It should be noted that although oxide phase was not detected in the consolidated Cu by X-ray diffraction, its existence with a small amount cannot be excluded. The addition of CNTs increased the thermal stability of the UFG Cu matrix as recrystallization was not observed in the composite samples up to 1000 K. For these specimens, the dislocation density remained unchanged up to about 500 K, then it decreased indicating a recovery of the microstructure. It is noted that in sample Cu-CNT-RT heated up to 1000 K the dislocation density remained as high as the value for the pure Cu specimens before annealing.

Conclusions

1. The Cu-CNT composite processed at RT exhibited a half as large mean grain size and a three times higher dislocation density than those observed in the specimens either consolidated from pure Cu powder or processed from bulk Cu by HPT. The small grain size and the pinning effect of CNT fragments on dislocations led to significant twin boundary formation during HPT.
2. The increase of the temperature of HPT-processing to 373 K resulted in a slight increase of the grain size, and a strong decrease of the dislocation density and the twin boundary frequency in the composite.

3. The measured flow stress agrees well with the value calculated by the Taylor-formula indicating that the CNT fragments strengthen the composite rather indirectly via the increase of the dislocation density.
4. The thermal stability of Cu consolidated from coarse powder particles by HPT was better than that for Cu processed from bulk coarse-grained material by HPT. This difference can be attributed to the usual contamination in materials produced by powder metallurgy. The addition of CNTs increased significantly the stability of the UFG Cu matrix.

Acknowledgements

This work was supported by the Hungarian Scientific Research Fund (OTKA) under Grant Nos. K81360 and K71594. The European Union and the European Social Fund have provided financial support to the project under the Grant Agreement No. TAMOP 4.2.1./B-09/KMR-2010-0003. HSK acknowledges the support of a Grant (B551179-08-01-00) from the cooperative research project "Development of common manufacturing technology for high functional susceptor" funded by the Ministry of Knowledge Economy, Republic of Korea. The authors thank Gábor Varga for performing SEM experiments.

References

[1] R.Z. Valiev, T.G. Langdon, Principles of equal-channel angular pressing as a processing tool for grain refinement, Prog. Mater. Sci. 51 (2006) 881-981.
[2] A.P. Zhilyaev, T.G. Langdon, Using high-pressure torsion for metal processing: Fundamentals and applications, Prog. Mater. Sci. 53 (2008) 893-979.
[3] H.J. Choi, J.H. Shin, B.H. Min, J.S. Park, D.H. Bae, Reinforcing effects of carbon nanotubes in structural aluminum matrix nanocomposites, J. Mater. Res. 24 (2009) 2610-2616.
[4] H. Li, A. Misra, Y. Zhu, Z. Horita, C.C. Koch, T.G. Holesinger, Processing and characterization of nanostructured Cu-carbon nanotube composites, Mater. Sci. Eng. A 523 (2009) 60-64.
[5] G. Ribárik, J. Gubicza, T. Ungár, Correlation between strength and microstructure of ball-milled Al–Mg alloys determined by X-ray diffraction, Mater. Sci. Eng. A 387–389 (2004) 343-347.
[6] L. Balogh, G. Ribárik, T. Ungár, Stacking Faults and Twin Boundaries in fcc Crystals Determined by X-ray Diffraction Profile Analysis, J. Appl. Phys. 100 (2006) 023512.
[7] P. Jenei, E.Y. Yoon, J. Gubicza, H.S. Kim, J.L. Lábár, T. Ungár, Microstructure and hardness of copper–carbon nanotube composites consolidated by High Pressure Torsion, Mater. Sci. Eng. A 528 (2011) 4690-4695.
[8] J. Luo, R. Stevens, Porosity-dependence of elastic moduli and hardness of 3Y-TZP ceramics, Ceram. Int. 25 (1999) 281-286.
[9] N.Q. Chinh, J. Gubicza, T.G. Langdon, Characteristics of face-centered cubic metals processed by equal-channel angular pressing, J. Mater. Sci. 42 (2007) 1594-1605.
[10] J. Gubicza, N.Q. Chinh, J.L. Lábár, Z. Hegedűs, C. Xu, T.G. Langdon, Microstructure and yield strength of severely deformed silver, Scr. Mater. 58 (2008) 775-778.
[11] D.H. Chung, W.R. Buessem, in: F.W. Vahldiek, S.A. Mersol (Eds.), Anisotropy of Single Crystal Refractory Compounds, vol. 2, Plenum Press, New York, 1968, pp. 217-245.
[12] N. Hansen, Hall–Petch relation and boundary strengthening, Scr. Mater. 51 (2004) 801-806.
[13] D.A. Hughes, N. Hansen, Microstructure and strength of nickel at large strains, Acta Mater. 48 (2000) 2985-3004.
[14] T. Tokunaga, K. Kaneko, Z. Horita, Production of aluminum-matrix carbon nanotube composite using high pressure torsion, Mater. Sci. Eng. A 490 (2008) 300-304.